Journal of Solid State Chemistry **150,** 363–370 (2000)
doi:10.1006/jssc.1999.8607, available online at http://www.idealibrary.com on IDEAL®

Use of X-Ray Absorption Spectra as a "Fingerprint" of the Local Environment in Complex Chalcogenides

C. Branci,[1] M. Womes,[2] P. E. Lippens,[3] J. Olivier-Fourcade,[3] and J. C. Jumas[3]

Laboratoire de Physicochimie de la Matière Condensèe, Université Montpellier II, C. C. O3 Place Eugene Bataillon, 34 095 Montpellier Cedex 05, France

Received July 14, 1999; in revised form December 2, 1999; accepted December 13, 1999

The local environment of tin, titanium, iron, and sulfur in spinel compounds $Cu_2FeSn_3S_8$ and $Cu_2FeTi_3S_8$ was studied by X-ray absorption spectroscopy (XAS) at the titanium, iron, sulfur K edges, and the tin L_I-edge. As detailed calculations of the electronic structure of these compounds are difficult to carry out due to the large number of atoms contained in the unit cell, the XAS spectra of the spinels are compared to those of relatively simple binary sulfides like SnS_2, TiS_2, and FeS. Indeed, the metal environments in these binary compounds are very similar to those in the spinels, and they can be considered good model compounds allowing the interpretation of electronic transitions observed in the spectra of quaternary phases. In the latter, the bottom of the conduction band is mainly formed by Sn 5*s*–S 3*p*, Sn 5*p*–S 3p antibonding states for the tin-based compounds and by Ti $3d_{t2g}$–S 3*p*, Ti $3d_{eg}$–S 3p antibonding states for the titanium-based compounds. It it shown that the local environment of iron atoms remains unchanged when substituting tin with titanium atoms, according to a topotactic substitution.

INTRODUCTION

Intensified efforts are currently made with regard to the search for new electrode materials for "Lithium-ion" batteries. Grade-one candidates for such electrodes are all compounds with crystal lattices providing a large number of vacant lattice or interstitial sites, an essential criterion when large amounts of lithium atoms are to be accommodated in the host lattice of the electrode. From this point of view, chalcogenide spinels are expected to be promising candidates for electrode materials in lithium and lithium-ion batteries (1–6). The cubic normal spinel $A[B_2]X_4$ (space group $Fd\bar{3}m$) has a three-dimensional lattice with A cations occupying the 8*a* tetrahedral sites, B cations on the 16*d* octahedral sites, and X anions in in a close packed (*ccp*) arrangement. Thus, a large number of sites (16*c* octahedral, and 8*b*, 48*f* tetrahedral sites) are empty and available for lithium intercalation, which explains the currently increasing interest in materials with spinel structure.

In a recent work, $Cu_2MSn_3S_8$ (M = Mn, Fe, Ni) thiospinels have been studied as cathodic material in lithium cells (7) and $Cu_2CoSn_3S_8$ as an anodic material in lithium-ion batteries (8). Moreover, regarding $Cu_2FeSn_3S_8$, it has been shown that substitution of tin by titanium atoms gives rise to an improvement of the specific capacity (9) allowing the use of $Cu_2FeSn_3S_8$ and $Cu_2FeTi_3S_8$ compounds as cathode materials in lithium cells.

The insertion mechanism in these spinel compounds is not precisely known. In order to elucidate this mechanism, a good understanding of the host material structure is necessary.

In this context, we carried out a study of the quaternary phases $Cu_2MSn_3S_8$ (M = Mn, Fe, Co, Ni) and the titanium-based compounds $Cu_2FeTi_xSn_{3-x}S_8$ (with $x = 0, 3/2, 3$) by means of X-ray absorption spectroscopy (XAS) at the S K, Sn L_I, Fe K, and Ti K-edges. The large number of atoms (56) contained in the unit cell does not allow a detailed theoretical calculation of the electronic structure of these compounds in order to interpret their absorption spectra. Instead, some binary compounds in which the metallic element are found in a similar environment were studied as a "fingerprint" of these arrangements.

These binary compounds are the disulfides of tin and titanium (SnS_2, TiS_2) and iron sulfide (FeS). In all these model compounds the metal atom is found in an octahedral environment MS_6. A comparison between the XAS spectra of the binary and spinel compounds has been achieved by a qualitative approach considering published theoretical calculations of the electronic structure of the binary compounds. The band structures of these model compounds are calculated using the tight-binding method (10, 11), and an excellent agreement between theoretical and experimental results was found (11). We dispose therefore of a reliable

[1] To whom correspondence should be addressed.

[2] Present address: Institut Français du Pétrole 1 et 4, avenue de Bois-Priau, 92 852 Rueil Malmaison Cedex, France.

[3] Present address: Laboratorie des Agrégats Moléculaire et Matériaux Inorganiques, Université Montpellier II, C. C. 15 Place Eugene Bataillon, 34 095 Montpellier Cedex 05, France.

0022-4596/00 $35.00

interpretation of X-ray absorption spectra that can now be transferred to more complex spectra.

EXPERIMENTAL

All the spinel compounds were prepared by solid state reaction. Mixed stoichiometric amounts of the elements were sealed in evacuated quartz tubes under vacuum ($P = 10^{-3}$ Pa). The mixture was heated to 300°C for 1 day, then the temperature was raised to a final constant value of 750°C for 10 days. In this way, black powders were obtained. The purity and the homogeneity of all compounds was examined by X-ray powder diffraction. Rietveld refinements of patterns were carried out and confirmed the spinel structure with copper on tetrahedral sites and all other metals on octahedral sites. TiS_2 and FeS were synthesized in the same way but with an annealing at 940° and 800°C, respectively. Tin disulfide SnS_2 was obtained by passing an H_2S flow through a solution of $SnCl_2$;$5H_2O$ in 3 M HCl (12). The crystallization of the precipitate was achieved by annealing at 400°C. X-ray powder diffraction of all binary compounds revealed that the reactions had been completed leading to the pure phases.

The X-ray absorption near edge structure (XANES) measurements were carried out using the synchrotron radiation of Super ACO (for the sulfur K-edge) and DCI (for Ti, Fe, Cu K-edges and Sn L_1-edge) storage rings at LURE (Orsay). The samples to be investigated were finely ground and passed through a 5-μm sieve in order to obtain powders being homogenous in particle size. At the S K-edge, a double-crystal monochromator equipped with Si(111) crystal pairs was used, giving a resolution of 0.4 eV. The samples were prepared by spreading the powders on adhesive tape fixed to an aluminum plate. The spectra were recorded in the total electron-yield mode. For all other edges, a thin membrane was coated with the powder. The recordings were carried out in the transmission mode. The beam line was equipped with a Si(311) two-crystal monochromator for the Fe and Ti-edges, allowing a resolution of 0.2 eV, and with a Si(111) monochomator for the Sn L_I-edge. The XAS spectra were treated as follows: the absorption background was subtracted supposing a linear behavior over the whole energy range, then the spectra were normalized to give the same absorption step amplitude in a range of pure atomic absorption, i.e., 10 eV above the absorption step.

RESULTS AND DISCUSSION

First, we present the XAS spectra of SnS_2, TiS_2, and FeS at the sulfur- and metal-absorption edges. The structural parameters of each binary and spinel compounds are presented in Table 1. The most common polytype of tin disulfide SnS_2 in 1T (space group $P\bar{3}m1$), with a repeating unit of two layers of close packed dichalcogenides and sandwiched tin cations in regular octahedral coordination (16). For the titanium disulfide TiS_2, a similar structure is observed. The cations in iron sulfide FeS, are equally found in octahedral coordination, however, the octahedron is strongly distorted (17).

Figure 1 shows the XAS spectrum SnS_2 at the sulfur K-edge (2472 eV), and Table 2 gives the positions of each features. The S K-edge reflects transitions from the S 1*s* core level to the S 3*p* empty levels. The peak (a) in Fig. 1

TABLE 1
Structural Parameters of SnS_2, TiS_2, FeS, and $Cu_2FeSn_3S_8$

Compounds	SnS_2[a]	TiS_2[b]	FeS[c]	$Cu_2FeSn_3S_8$[d]
Space group	$P\bar{3}m1$	$P\bar{3}m1$	$P\bar{6}2c$	$Fd\bar{3}m$
Number of coordinataion for the metallic element	6	6	6	Cu : 4 Fe, Sn : 6
Sites	Sn(1*a*) S(2*d*)	Ti(1*a*) S(2*d*)	Fe(12*i*) S1(2*a*) S2(4*f*) S3(6*h*)	Cu(8*a*) Fe, Sn(16*d*) S(32*e*)
Distances metallic-sulfur	d(Sn–S) = 2.56 Å	d(Ti–S) = 2.43 Å	$d1$ = 2.35 Å $d2$ = 2.44 Å $d3$ = 2.50 Å $d4$ = 2.51 Å $d5$ = 2.64 Å $d5$ = 2.44 Å	d(Cu–S) = 2.34 Å $d6$[e] = 2.51 Å

[a] From J. Oftedal (13).
[b] From R. R. Chianelli *et al.* (14).
[c] From F. Bertaut (15).
[d] This work
[e] Average distance between the Sn–S and Fe–S bonds.

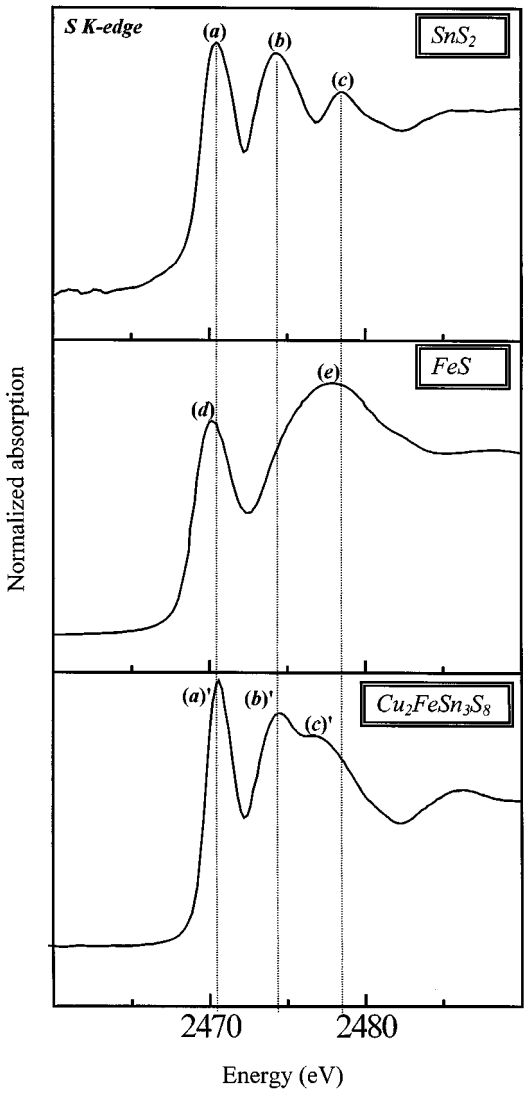

FIG. 1. X-ray absorption spectra at S K-edge for SnS_2, FeS, and $Cu_2FeSn_3S_8$.

represents transitions to antibonding states made up of S 3*p* states mixed with the Sn 5*s* states. The second peak (b) in Fig. 1 is due to antibonding states made up of S 3*p* states mixed with the Sn 5*p* states. A comparison with a tight binding calculation of the electronic band structure (10) confirms these two attributions. The last feature (c) in Fig. 1, lying beyond the energy range accessible by the tight binding approach is probably due to S 3*p*–Sn 5*d* interactions. The first peak (d) in Fig. 1 of the FeS XAS spectrum can be assigned to the antibonding states formed by S 3*p* interacting with Fe 3*d* states, the second broad peak (e) in Fig. 1 to mixed S 3*p*–Fe 4*s* and S 3*p*–Fe 4*p* states. The large width of this latter peak can be explained by the large number of transitions observed within this peak (11). Finally, the XAS spectrum of TiS_2 at sulfur K-edge is presented in Fig. 2. The spectrum can be interpreted in the following way (18): the first two peaks ((f) and (g) in Fig. 2) are assigned to transitions to sulfur 3*p* states mixed with titanium $3d_{t2g}$ and $3d_{eg}$ levels, respectively. The crystal field splitting of about 2 eV derived from the XAS spectrum is in agreement with previous studies (19–20). The peak labeled (h) in Fig. 2 is due to interactions between the suflur 3*p* orbital and the Ti 4*s* and 4*p* orbitals and constitutes a kind of continuum of accessible states. In order to study the local environment of the metal in TiS_2 and SnS_2 binary compounds, we carried out XAS measurements at the titanium K-edge and the tin L_I-edge, respectively. Figure 3a shows the SnS_2 absorption spectrum at the Sn L_I-edge (4465 eV). This edge reflects transitions from the Sn 2*s* core level to the lowest empty

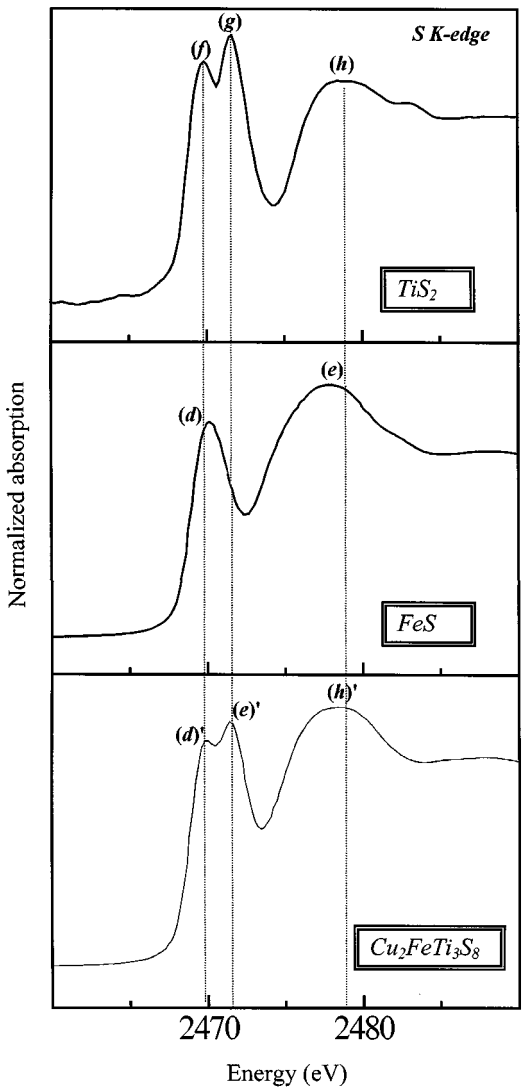

FIG. 2. X-ray absorption spectra at S K-edge for TiS_2, FeS, and $Cu_2FeTi_3S_8$.

TABLE 2
Position of the XAS Peaks

Compounds		*E*	Electronic transition *italic*: obtained in the literature
	(*a*)	2470.4	*S 1s* → *S 3p Sn 5s* σ*
SnS_2	(*b*)	2474.2	*S 1s* → *S 3p Sn 5p* σ*
	(*c*)	2478.3	
FeS	(*d*)	2470.1	*S 1s* → *S 3p Fe 3d* σ*t*
	(*e*)	2477.5	*S 1s* → *S 3p Fe 4s* σ* and *S 3p Fe* 4*p* σ*
	(*g*)	2469.5	*S 1s* → *S 3p Ti* $3d_{t2g}$ σ*
TiS_2	(*h*)	2471.5	*S 1s* → *S3p Ti* $3d_{eg}$ σ*
	(*i*)	2478.0	*S 1s* → *S 3p Ti 4s* σ* and *S 1s* → *S 3p Ti 4p*
	(*a*)′	2470.5	S 1*s* → S 3*p* Sn 5*s* σ* and S 3*p* Fe 3*d* σ*
$Cu_2FeSn_3S_8$	(*b*)′	2474.3	S 1*s* → S 3*p* Sn 5*p* σ*
	(*c*)′	2477.5	S 1*s* → S 3*p X* 4*s* σ*, S 3*p X* 4*p* σ*[a] and S 1*s* → S 3*p* Sn 5*d* σ*
	(*d*)′	2469.7	S 1*s* → S 3*p* Ti $3d_{t2g}$ σ* and S 3*p* Fe 3*d* σ*
$Cu_2FeTi_3S_8$	(*e*)′	2471.5	S 1*s* → S 3*p* Ti $3d_{eg}$ σ*
	(*f*)′	2477.4	S 1*s* → S 3*p Y* 4*s* σ* and S 3*p Y* 4*p* σ*[b]

Note. *E* represents the position (eV).
[a] *X* = Fe, Cu.
[b] *Y* = Fe, Cu, Ti.

states of *p* character of the probed atom. As the environment of tin atoms in SnS_2 is a regular octahedron formed by six Sn–S bonds with the same length (16), no splitting of the tin 5*p* states occurs. As a consequence, a highly symmetric white line is observed due to electronic transitions from Sn 2*s* to Sn 5*p*–S 3*p* antibonding states. The XAS spectrum of TiS_2 at the titanium K-edge (4965 eV) is presented in Fig. 3b. Or results agree with those published previously (21). The main absorption step corresponds to the transition Ti 1*s* → Ti 4*p*–S 3*p* antibonding states and the origin of the small peak in the pre-edge region is not precisely known. It may be due to either a transition to Ti 3*d* levels, allowed by a partial quadrupolar character of the transition (22), or to a small fraction of Ti 4*p* orbitals, which were found at this energy by a band structure calculation (21), or both.

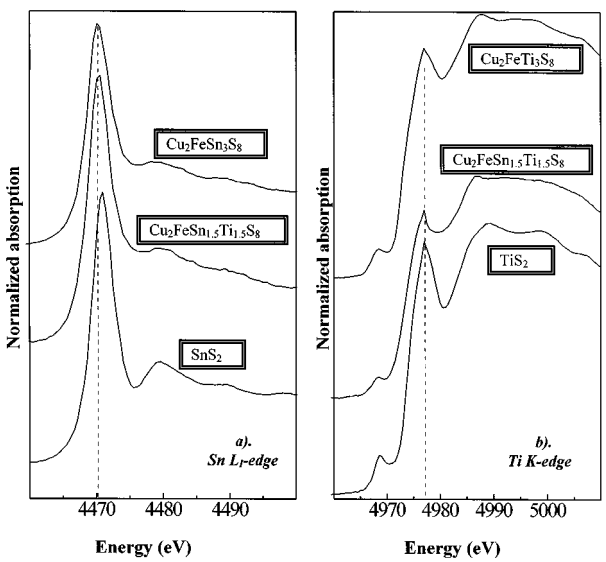

FIG. 3. X-ray absorption spectra at (a) Sn L_I-edge and (b) Ti K-edge for $Cu_2FeTi_xSn_{3-x}S_8$, TiS_2, and SnS_2.

Let us now turn to the characterization of the spinel compounds. A study of the local environment of tin atoms by ^{119}Sn Mössbauer spectroscopy was carried out previously (9, 23), confirming that tin atoms are in the formal oxidation state (IV) in a slightly distorted octahedral environment. The substitution of tin by titanium atoms leads to an increase of the isomer shift which can be related to an increase of the covalent character of the Sn–S bonds with increasing amounts of titanium in the spinels (23).

In order to study the band structure above the Fermi energy and to characterize the local environment of the sulfur atoms of $Cu_2MSn_3S_8$ (M = Mn, Fe, Co, Ni), some XAS measurements were carried out at the S K-edge. As XAS reflects the partial densities of unoccupied states (DOS), the knowledge of the local environment of the probing atom is essential for a detailed analysis of XAS spectra. Figure 4 shows the first neighbors of sulfur atoms in the spinel compound $Cu_2FeSn_{23}S_8$ and the Table 1 gives the sulfur–metal distances. $Cu_2MSn_3S_8$ (M = Mn, Fe, Co, Ni) XAS spectra are presented in Fig. 5. The spectra of the four compounds are very similar in shape showing that a change of the transition element has a minor influence on the electronic structure. Only the spectrum of $Cu_2FeSn_3S_8$ was compared with the binary compounds spectra (Fig. 1). The first peak labeled (a)′ in Fig. 1 is found at the same energy as

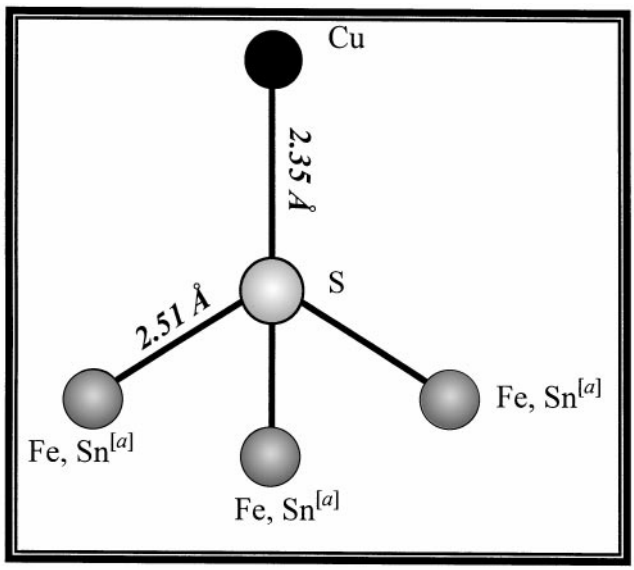

FIG. 4. Local environment of sulfur atoms in $Cu_2FeSn_3S_8$ spinel. [a]: statistic occupation: 3Sn/1Fe.

for SnS_2 and FeS (respectively labeled (a) and (d) and can, therefore, be attributed to the electronic transitions S $1s \rightarrow$ Sn $5s$–S $3p$ antibonding states and S $1s \rightarrow$ S $3p$–Fe $3d$ antibonding states. Because of the greater number of tin atoms as compared to the iron atoms in the compound (3 Sn/1 Fe), this peak predominantly reflects the admixture of S $3p$ states with the tin orbitals. The second peak (b)′ in Fig. 1 at 2473.5 eV coincides energetically with the second peak of SnS_2 (b) and can be thus explained by a transition S $1s \rightarrow$ Sn $5p$ S $3p$ antibonding states. Finally, the second peak of FeS (e) and the third peak (c) of SnS_2 coincide with the third (c)′ of $Cu_2FeSn_3S_8$. This latter is therefore due to the electronic transitions S $1s \rightarrow$ S $3p$ Fe $4s$ antibonding states, S $1s$–S $3p$ Fe $4p$ antibonding states and S $1s \rightarrow$ S $3p$ Sn $5d$ antibonding states. The large width observed for this feature can be explained by the large number of transitions observed. Regarding the contribution of copper states, the atomic energies of the Cu $4s$ and $4p$ states were found to be lower energy than those of the Fe $4s$ and $4p$ states (24), respectively. This leads to antibonding Cu–S states at energy lower than those of the antibonding Fe–S states. However, the energy difference between these two antibonding states should be reduced by the effect of interatomic distances: the Cu–S bonds are smaller than the Fe–S bonds (Table 1). Thus, the Cu–S and Fe–S antibonding states are expected to be in the same energy range and should both contribute to XAS peak labeled (c)′ in Fig. 1.

The substitution of tin by titanium atoms in spinel compounds concerns the octahedral sites. In order to characterize the titanium environment, a comparison of the XAS spectra obtained for TiS_2 and the titanium-based spinel at the sulfur K-edge was carried out. The $Cu_2FeTi_3S_8$ XAS spectrum is presented in Fig. 2. Again, the comparison of the TiS_2 and FeS spectra with those of $Cu_2FeTi_3S_8$ can help us to interpret the spinel spectrum. The first peak labeled (d)′ in Fig. 2 is due to the transitions of S $3p$ states hybridized with Ti $3d(t2g)$ while the second peak (e)′ is mainly attributed to a transition to S $3p$ states hybridized with Ti $3d(eg)$. These transitions can be considered predominant as compared to those derived from iron orbitals. The large peak (f)′ in Fig. 2 at 2477.4 eV, includes a large number of electronic transitions. In this energy range, we find transitions to S $3p$ respectively mixed with Fe $4s$, Fe $4p$, Ti $4s$, Ti $4p$, Cu $4s$, Cu $4p$ states.

Finally, the large number of electronic transitions that are to be taken into account for the $Cu_2FeTi_{1.5}Sn_{1.5}S_8$ spinel compound does not allow a simple decomposition of its XAS spectrum. Nevertheless, this spectrum is presented in Fig. 6 and shows the same basic features as those of the spinel compounds.

In addition to the investigation of the sulfur K-edge, a study of the tin, titanium, and iron edges has been carried out. Because of similarity of the XAS spectra obtained for all transition elements (Mn, Fe, Co, Ni), only the XAS spectra

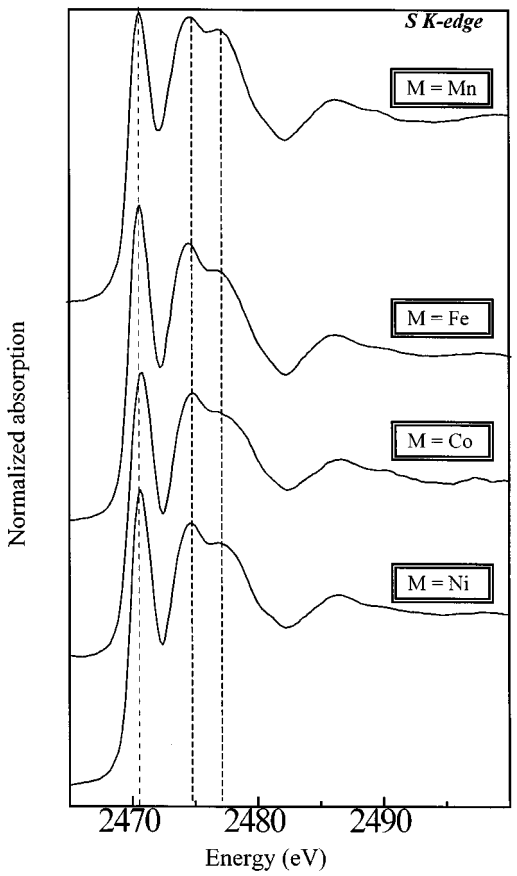

FIG. 5. X-ray absorption spectra at S K-edge of $Cu_2MSn_3S_8$ (M = Mn, Fe, Co, and Ni).

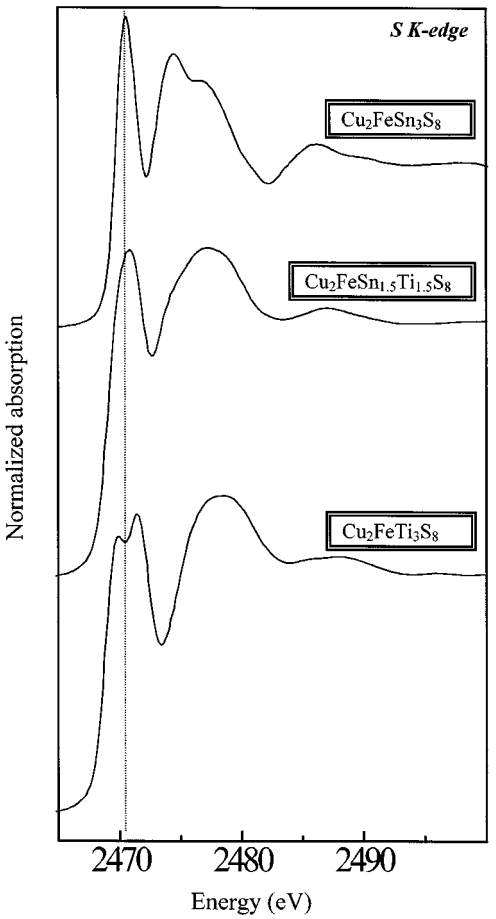

FIG. 6. X-ray absorption spectra at S K-edge of iron-based spinels compounds.

of the iron spinel are shown in this paper. Figure 3a shows the Sn L_I-edges of $Cu_2FeSn_3S_8$ and $Cu_2FeTi_{1.5}Sn_{1.5}S_8$ reflecting transition from the Sn 2*s* core level to the unoccupied Sn 5*p* states. A comparison of these spectra with that of SnS_2 suggests the similarity of the local environment for the tin atoms, in agreement with the presence of SnS_6 octahedra in the spinel compounds. The small shift in the energy position of the white line for the spinels (4470.2 eV for $Cu_2FeSn_3S_8$, 4471 eV for SnS_2) could be due to the difference in the coordination of sulfur ions around the tin sites. Thus the white line observed in the spectra of the spinels is mainly due to transitions from Sn 2*s* level to the Sn 5*p*–S 3*p* antibonding states.

The titanium K-edge spectra are presented in Fig. 3b. There is no noticeable differences between the spinel XAS spectra, confirming a similar titanium environment for each of the substituted compounds. A comparison of the peak positions with those of TiS_2 allows three conclusions to be derived: (i) the similarity of spectra confirms the presence of TiS_6 octahedra in the quaternary phases; (ii) the close values of absorption edge positions suggest that no important changes take place in the Ti–S bond length in quaternary compounds (2.50 Å) compared to TiS_2 (2.43 Å); (iii) all interpretations of the spectral structures in terms of electronic transitions can be derived from the binary compounds.

The Fe K-edge (7112 eV) reflects transitions from the iron core level 1*s* to empty levels with Fe 4*p* character. The similarity of the spectra shown in Fig. 7 confirms the existence of similar iron environments in tin-based as well as titanium-substituted spinels; i.e., the environment of iron atoms is not affected by this substitution. Our spectra of both spinel compounds agree well with that obtained earlier for the iron sulfides FeS, and give rise to a similar interpretation (11). The first derivative of the $Cu_2FeSn_3S_8$ spectrum presented in Fig. 8 can help us in order to interpret the spectrum of $Cu_2FeSn_3S_8$ (11). Figure 8 shows several main features labeled A, B, and C. In the spinel compound the iron environment is in a distorted octahedron (25). A compression in [111] direction of the FeS_6 polyhedra leads to a partial splitting of the Fe 4*p* states into a singlet and

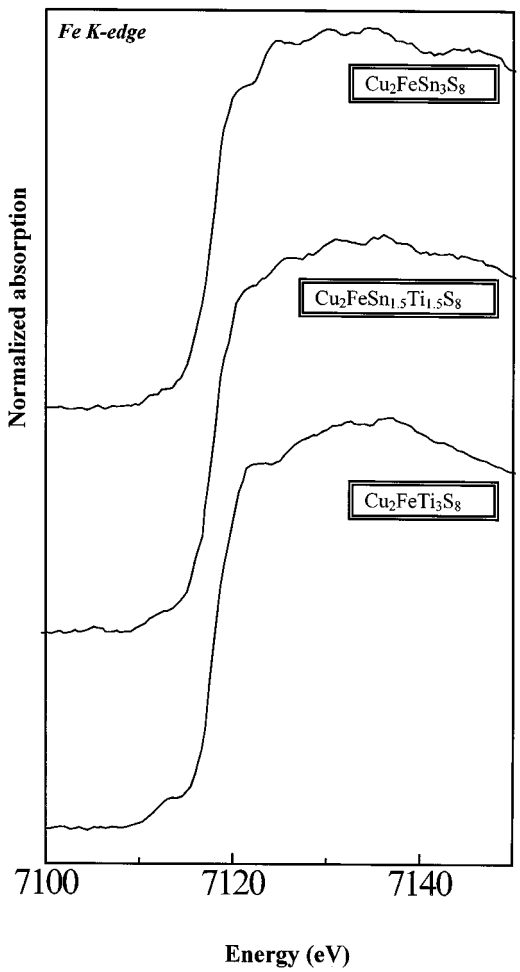

FIG. 7. X-ray absorption spectra at Fe K of $Cu_2FeTi_xSn_{3-x}S_8$.

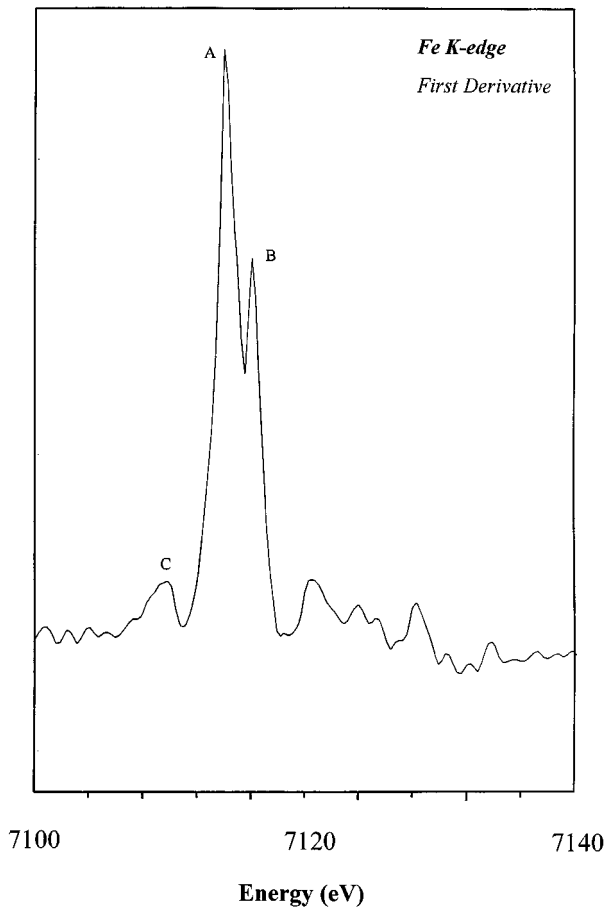

FIG. 8. First derivative of X-ray absorption $Cu_2FeSn_3S_8$ spectra at the S K-edge.

a doublet. Therefore, the features A and B can be interpreted as a transition to these singlet and doublet, in the main absorption step. The same distortion leads to an admixture of the Fe 4*p* orbital to the Fe 3*d* state and gives rise to the prepeak labeled C. The latter feature is then characteristic of FeS_6 octahedra, according to the structural consideration where the iron is in distorted octahedral site.

CONCLUSION

X-ray absorption spectroscopy can be used to characterize the local environment in compounds presenting a complex structure (spinel structure). In order to interpret XAS spectra a full calculation of the electronic band structure is not necessary, but a comparison with binary compounds allows us to analyze the shape of more complex structures such as spinel. At the sulfur K-edge, the bottom of the conduction band of $Cu_2FeSn_3S_8$ is principally made by an admixture between sulfur 3*p* orbitals with tin orbitals (5*s* and 5*p*). For the titanium-based compounds $Cu_2FeTi_3S_8$ the Ti $3d_{t2g}$ and Ti $3d_{eg}$ orbitals predominate the bottom of conduction band.

Regarding tin L_I-edge and titanium K-edge, we observed a great similarity between the spectra of spinels and binary sulfides (SnS_2 and TiS_2) indicating that they have, respectively, a similar environment of tin and titanium atoms. At the iron K-edge, we have used the derivative of the XAS spectrum in order to show the different electronic transitions. The complexity of the spectrum is mainly due to a splitting of Fe 4*p* orbitals into one singlet and one doublet. This interpretation agrees with those of FeS spectra (11).

Finally, at all the XAS metal-edges, the substitution of tin by titanium atoms occurs without any important change in spectra of the spinels, confirming thus a topotactic substitution in good agreement with the Rietveld analysis of their X-ray diffraction patterns (23). The interpretations of the various structures observed in the absorption spectra especially those given for the rather complex sulfur K-edge, can now be used for an assignment of the structures observed in the spectra of other complex sulfides compounds.

ACKNOWLEDGMENTS

The authors thank A. M. Flank and P. Lagarde for their help in collecting data of Super-Aco, and F. Villian, Ph. Parent, and R. Cortes for DCI experiments.

REFERENCES

1. M. Eisenberg, *J Electrochem. Soc.* **127,** 2382 (1980).
2. A. C. W. P. James, J. B. Goodenough, and N. J. Clayden, *J. Solid State Chem.* **77,** 356 (1988).
3. M. M. Thackeray, *J. Electrochem. Soc.* **142**(8), 2558 (1995).
4. G. Pistoria, D. Zane, and Y. Zhang. *J. Electrochem. Soc.* **142**(8), 2551 (1995).
5. M. L. Elidrissi-Moutbassim, J. Olivier-Fourcade, J. Senegas, and J. C. Jumas, *Mater. Res. Bull.* **25,** 1083 (1993).
6. J. Morales, J. L. Tirado, M. L. Elidrissi-Moutbassim, J. Olivier-Fourcade, and J. C. Jumas, *J. Alloys Compounds* **217,** 176 (1995).
7. P. Lavela, J. L. Tirado, J. Morales, J. Olivier-Fourcade, and J. C. Jumas, *J. Mater. Chem.* **6**, 41 (1996).
8. M. A. Cochez, J. C. Jumas, P. Lavela, J. Morales, J. Olivier-Fourcade, and J. L. Tirado, *J. Power Sources* **62,** 99 (1996).
9. C. Branci, J. Sarradin, J. Olivier-Fourcade, and J. C. Jumas, *Mol. Cryst. Liq. Cryst.* **311,** 69 (1998).
10. I. Lefebvre, M. Lannoo, J. Olivier-Fourcade, and J. C. Jumas, *Phys. Rev. B.* **44,** 1004 (1991).
11. M. Womes, R. C. Karnatak, J. M. Esteva, L. Lefebvre, G. Allan, J. Olivier-Fourcade, and J. C. Jumas. *J. Phys. Chem. Solids* **58**(2), 345 (1997).
12. J. C. Jumas, thesis, Université Montpellier II, 1975.
13. J. Oftedal, *Z. Phys. Chem.* **137,** 301 (1928).
14. R. R. Chianelli, J. Scanlon, and A. H. Thompson, *Mater. Res. Bull.* **10,** 256 (1975).
15. F. Bertaut, *Bull. Fr. Minér. Crist.* **79,** 256 (1956).
16. A. A. Bachin, "Crystallography and Crystal Chemistry of Materials with Layered structure" (F. Lévy, Ed.). Reidel, Dordrecht, 1976.
17. A. F. Andresen, *Acta. Chem. Scand.* **14,** 919 (1960).

18. Z. Y. Wu, G. Ouvrard, S. Lermaux, P. Moreau, P. Gressier, F. Lemoigno, and J. Rouxel, *Phys. Rev. Lett*. **77**(10), 2101 (1996).
19. D. W. Fisher, *Phys. Rev. B* **8** (1973).
20. C. Suguira, S. Shoji, and Kojima, *Jpn. J. Appl. Phys*. **30,** 1742 (1991).
21. P. Moreau, G. Ouvrad, P. Gressier, P. Ganal, and J. Rouxel, *J. Phys. Chem. Solids* **57,** 1117 (1996).
22. F. Farges, *Non-Cryst. Solids* **204,** 53 (1996).
23. C. Branci, J. Olivier-Fourcade, J. C. Jumas, P. Lavela, C. Perez, and J. L. Tirado, *Chem. Mater*. **11,** 2687 (1999).
24. F. Herman and S. Skillman, "Atomic Structure Calculations." Prentice–Hall, Englewood Cliffs, NJ, 1963.
25. J. Padiou, J. C. Jumas, and M. Ribes, *Rev. Chim. Minér*. **18,** 33 (1981).